THE JOURNAL OF BIOLOGICAL CHEMISTRY
Vol. 279, No. 52, Issue of December 24, pp. 54304–54311, 2004
Printed in U.S.A.

Molecular Determinants in TRPV5 Channel Assembly*

Received for publication, June 4, 2004, and in revised form, October 14, 2004
Published, JBC Papers in Press, October 15, 2004, DOI 10.1074/jbc.M406222200

Qing Chang, Emmanouela Gyftogianni, Stan F. J. van de Graaf, Susan Hoefs, Freek A. Weidema, René J. M. Bindels, and Joost G. J. Hoenderop‡

From the Department of Physiology, Nijmegen Center for Molecular Life Sciences, Radboud University Nijmegen Medical Center, NL-6500 HB Nijmegen, The Netherlands

The epithelial Ca^{2+} channels TRPV5 and TRPV6 mediate the Ca^{2+} influx in 1,25-dihydroxyvitamin D_3-responsive epithelia and are therefore essential in the maintenance of the body Ca^{2+} balance. These Ca^{2+} channels assemble in (hetero)tetrameric channel complexes with different functional characteristics regarding Ca^{2+}-dependent inactivation, ion selectivity, and pharmacological block. Glutathione *S*-transferase pull-downs and co-immunoprecipitations demonstrated an essential role of the intracellular N- and C-tails in TRPV5 channel assembly by physical interactions between N-N tails, C-C tails, and N-C-tails. Patch clamp analysis in human embryonic kidney (HEK293) cells and $^{45}Ca^{2+}$ uptake experiments in *Xenopus laevis* oocytes co-expressing TRPV5 wild-type and truncated proteins indicated that TRPV5ΔN (deleted N-tail) and TRPV5ΔC (deleted C-tail) decreased channel activity of wild-type TRPV5 in a dominant-negative manner, whereas TRPV5ΔNΔC (deleted N-tail/C-tail) did not affect TRPV5 activity. Oocytes co-expressing wild-type TRPV5 and TRPV5ΔN or TRPV5ΔC showed virtually no wild-type TRPV5 expression on the plasma membrane, whereas co-expression of wild-type TRPV5 and TRPV5ΔNΔC displayed normal channel surface expression. This indicates that TRPV5 trafficking toward the plasma membrane was disturbed by assembly with TRPV5ΔN or TRPV5ΔC but not with TRPV5ΔNΔC. TRPV5 channel assembly signals were refined between amino acid positions 64–77 and 596–601 in the N-tail and C-tail, respectively. Pull-down assays and co-immunoprecipitations demonstrated that N- or C-tail mutants lacking these critical assembly domains were unable to interact with tails of TRPV5. In conclusion, two domains in the N-tail (residues 64–77) and C-tail (residues 596–601) of TRPV5 are important for channel subunit assembly, subsequent trafficking of the TRPV5 channel complex to the plasma membrane, and channel activity.

TRPV5 and TRPV6 constitute the Ca^{2+} influx pathway in 1,25-dihydroxyvitamin D_3-responsive epithelia, including small intestine, kidney, and placenta, and play a vital role in the process of Ca^{2+} (re)absorption (1–4). Both channels belong to a distinct subfamily (TRPV) within the superfamily of transient receptor potential channels (TRP).[1] The TRP family consists of a diverse group of non-voltage-gated cation channels, including TRPC (canonical), TRPM (melastatin), and TRPV (vanilloid) subfamilies, which varies significantly in their selectivity and mode of activation (5). The understanding of the function, gating, regulation, and structure assembly of the TRP family is developing rapidly. Initially, it was demonstrated that the *Drosophila* TRP and TRPL members form heteromultimeric channels associated in a supramolecular signaling complex with specific receptors and regulators (6). Moreover, it has been identified that there are many channel compositions within the TRPC family, *e.g.* TRPC1/3, TRPC1/5, TRPC4/5, and TRPC3/6/7 (7–9). Within the TRPV family, the oligomeric structure of TRPV1 was studied by biochemical cross-linking, and the predominant existence of tetramers was suggested (10). More recently, it has been reported that TRPV5 and TRPV6 form homo- or heterotetramers in order to generate a pleiotropic set of functional channels with different Ca^{2+} transport (11–13). TRPV5 and TRPV6 share 75% sequence homology at the amino acid level (11–13) and display several similar functional properties, including the permeation profile for monovalent and divalent cations (14) and regulation by calciotropic hormones (15–21). However, detailed sequence comparison of the N- and C-tails of the TRPV5 and TRPV6 channels reveals significant differences, which may account for the unique electrophysiological properties including differences of inactivation, kinetic properties, and affinity for the blocker ruthenium red between these two homologous channels (22).

A considerable amount of information in channel subunit assembly has been accumulated by studies on voltage-gated K^+ (K_v) channels that are structurally related to the TRP channels. Previous studies indicated that the subfamily of Shaker-related K_v channels possesses a T1 domain in the N-tail, which confers subfamily specificity and inter-subunit assembly (23). This highly conserved T1 domain has been shown to spontaneously form tetramers in the absence of transmembrane sequences (24, 25). Crystallization of this domain further verified the reported biochemical and functional data and implicated that T1 is also involved in channel gating (25, 26). To date, no information is available about assembly domains in TRP proteins. Because TRPV5 shares common structural features with K_v channels, we hypothesized that there is at least one assembly signal within this channel.

The aim of the present study was to identify the regions in TRPV5 involved in channel assembly. By using different experimental approaches, including pull-down, co-immunoprecipitation, patch clamp, and immunocytochemical analysis, two

* This work was supported by the Dutch Organization of Scientific Research Grant Zon-Mw 016.006.001 and the Dutch Kidney Foundation Grant C03.6017. The costs of publication of this article were defrayed in part by the payment of page charges. This article must therefore be hereby marked "*advertisement*" in accordance with 18 U.S.C. Section 1734 solely to indicate this fact.

‡ To whom correspondence should be addressed: 160 Physiology, Radboud University Nijmegen Medical Center, P.O. Box 9101, NL-6500 HB Nijmegen, The Netherlands. Tel.: 31-24-3610571; Fax: 31-24-3616413; E-mail: J.Hoenderop@ncmls.ru.nl.

[1] The abbreviations used are: TRP, transient receptor potential; GST, glutathione *S*-transferase; HA, hemagglutinin; TRPC, TRP canonical; TRPV, TRP vanilloid; HA, hemagglutinin; RT, room temperature; PMSF, phenylmethylsulfonyl fluoride; NFDM, non-fat dried milk; MES, 2-(*N*-morpholino)ethanesulfonic acid; ANK, ankyrin.

critical domains in the N-tail and C-tail were identified to be involved in TRPV5 channel assembly and subsequent trafficking to the plasma membrane.

EXPERIMENTAL PROCEDURES

DNA Constructs and cRNA Synthesis—The N- and C-tails of TRPV5 were amplified and tagged with an HA or FLAG tag, respectively, by the use of PCR on the full-length cDNA of TRPV5, and were subsequently cloned into the pGEX 6p-2 (Amersham Biosciences) vector and the pT7Ts *Xenopus laevis* oocytes expression vector (27). (For HA-tagged TRPV5 N-tail, forward primer 5′-ATGTACCCATACGACGTGCCAGACTACGCAGGGGCCTGTCCACCCAAGG-3′ and reverse primer 5′-TTAAGGCCGCCCGTATTTCTTC-3′ were used. For FLAG-tagged TRPV5 N-tail, forward primer 5′-ATGGACTACAAGGATGACGATGACAAGGGGCCTGTCCACCCAAGG-3′ and reverse primer 5′-TTAAGGCCGCCCGTATTTCTTC-3′ were used. For HA-tagged TRPV5 C-tail, forward primer 5′-ATGTACCCATACGACGTGCCAGACTAC-GCAGGCGACACTCACTGGCGGG-3′ and reverse primer 5′-TCAGAAATGGTAGACTTCC-3′ were used. For FLAG-tagged TRPV5 C-tail, forward primer 5′-ATGGACTACAAGGATGACGATGACAAGGGCGACACTCACTGGCGGG-3′ and reverse primer 5′-TCAGAAATGGTAGACTTCC-3′ were used.) TRPV5 truncated proteins in which the N-tail (TRPV5ΔN), C-tail (TRPV5ΔC), or both tails (TRPV5ΔNΔC) were deleted were obtained by PCR and cloned into the pCINeo/IRES-GFP vector and subcloned into the pT7Ts vector (21). Deletion mutants of the assembly domain in the N-tail (deleted amino acids 64–76) or the C-tail (deleted amino acids 595–600) were obtained by *in vitro* mutagenesis and subcloned into the PT7Ts vector. (For N-tail deletion, forward primer 5′-CTGCGTCTCCTTAAGATAGCTGTGGGGGAGACGGCG-3′ and reverse primer 5′-CGCCGTCTCCCCCACAGCTATCTTAAGGAGACGCAG-3′ were used. For C-tail deletion, forward primer 5′-GTTGTGGCCACCACCGTGATGCCTCGCTTCCTGTGG-3′ and reverse primer 5′-CCACAGGAAGCGAGGCATCACGGTGGTGGCCACAAC-3′ were used.) pT7Ts constructs were linearized, and cRNA was synthesized *in vitro* as described previously (21). All constructs were verified by sequence analysis.

Electrophysiology—The full-length cDNA encoding wild-type TRPV5, TRPV5ΔN, TRPV5ΔC, and TRPV5ΔNΔC were transfected in HEK293 cells as described previously (22, 28). Currents using the whole-cell configuration were measured with an EPC-9 (HEKA Elektronik, Lambrecht, Germany; 8-pole Bessel filter, 10 kHz). Electrode resistances were between 2 and 5 megohms; capacitance and series resistance were compensated, and access resistance was monitored continuously. The step protocol consisted of 3-s voltage steps to −100 mV from a holding potential of +70 mV. The standard extracellular solution contained 150 mM NaCl, 1 mM $CaCl_2$, 6 mM CsCl, 1 mM $MgCl_2$, 10 mM glucose, and 10 mM HEPES/CsOH (pH 7.4). Monovalent cation currents were measured in nominally Ca^{2+}- and Mg^{2+}-free solution (free Ca^{2+} concentration is 10 nM), and Ca^{2+} currents in 1 mM $CaCl_2$ but Mg^{2+}-free solutions. Monovalent cation currents were inhibited by replacing 150 mM NaCl with an equimolar amount of *N*-methyl-D-glucamine-Cl. The standard internal (pipette) solution contained the following: 20 mM CsCl, 100 mM cesium aspartate, 1 mM $MgCl_2$, 10 mM 1,2-bis(2-aminophenoxy)ethane-*N*,*N*,*N*′,*N*′-tetraacetic acid, 4 mM Na_2ATP, and 10 mM HEPES/CsOH (pH 7.2). Cells were kept in a nominally Ca^{2+}-free medium to prevent Ca^{2+} overload and were exposed for a maximum of 5 min to a Krebs solution containing 1.5 mM Ca^{2+} before sealing the patch pipette to the cell. All experiments were performed at room temperature (RT; 20–22 °C).

GST Fusion Proteins and Pull-down Assay—PGEX6p-2 constructs were transformed in *E. coli* BL21, and GST-fused proteins were expressed and purified as described previously (21). Proteins of full-length TRPV5, TRPV5 N-tail, C-tail, or N- and C-tail deletion mutants were translated *in vitro* with [^{35}S]methionine (ICN Biomedicals Irvine, CA) for 120 min at 30 °C using rabbit reticulocyte lysates (Promega, Madison, WI). *In vitro* translated proteins were added to purified GST-fused truncated proteins, immobilized on glutathione-Sepharose 4B beads (Amersham Biosciences). After 2 h of incubation at RT, the beads were washed extensively with pull-down buffer (20 mM Tris-HCl (pH 7.4), 140 mM NaCl, 1 mM $CaCl_2$, 0.2% (v/v) Triton X-100, 0.2% (v/v) Nonidet P-40), and bound proteins were eluted with SDS-PAGE loading buffer and separated on SDS-polyacrylamide gels. Following electrophoresis, gels were analyzed by autoradiography (21).

Injection of Oocytes and Total Membrane Isolation—X. laevis oocytes were prepared and injected as described previously (21). To isolate total lysates, 20 oocytes were homogenized in 200 μl of homogenization buffer (HBA) (20 mM Tris-HCl (pH 7.4), 5 mM $MgCl_2$, 5 mM NaH_2PO_4, 1 mM EDTA, 80 mM sucrose, 1 mM PMSF, 10 μg/ml leupeptin, and 10 μg/ml pepstatin) and centrifuged twice at 100 × *g* for 10 min at 4 °C to remove yolk proteins. Next the total lysates were taken up in Laemmli buffer (2 μl/oocyte) at 37 °C for 30 min (2, 22, 29).

Immunoblot Analysis—Total lysates were subjected to SDS-PAGE (12–16% w/v) and blotted onto polyvinylidene difluoride membranes (Millipore Corp. Bedford, MA). Blots were incubated with 5% (w/v) non-fat dried milk (NFDM) in TBS-T (Tris-buffered saline (pH 7.4) containing 0.2% (v/v) Tween 20). Immunoblots were incubated overnight at 4 °C with mouse anti-HA (1:4000) or mouse anti-FLAG (1:8000) antibodies (Sigma), in 1 or 5% (w/v) NFDM in TBS-T, respectively. After washing, immunoblots were incubated at RT with the corresponding secondary antibody sheep anti-mouse IgG peroxidase (Sigma), (1:2000) in TBS-T. For co-immunoprecipitation assays, immunoblots were incubated overnight at 4 °C with mouse anti-FLAG peroxidase-coupled antibody (1:2000) (Sigma), 5% (w/v) NFDM in TBS-T. Immunopositive bands were visualized by using an enhanced chemiluminescence system (Pierce).

Co-immunoprecipitation—Twenty-microliter equivalents of protein A-coupled agarose beads (Amersham Biosciences) were preincubated for 3 h at RT with 2 μl of monoclonal anti-HA antibody (Sigma) in 0.7 ml of IPP500 (500 mM NaCl, 10 mM Tris (pH 8.0), 0.1%(v/v) Nonidet P-40, 0.1%(v/v) Tween 20, 1 mM PMSF, 10 μg/ml leupeptin, 10 μg/ml pepstatin) and 0.1%(w/v) bovine serum albumin. The beads were washed three times with IPP100 (100 mM NaCl, 10 mM Tris (pH 8.0), 0.1% (v/v) Nonidet P-40, 0.1% (v/v) Tween 20, 1 mM PMSF, 10 μg/ml leupeptin, 10 μg/ml pepstatin). Thirty oocytes were co-injected (each 12.5 ng) with HA- and FLAG-tagged TRPV5 N-tail or C-tail cRNA or cRNA transcribed from the deletion mutants. Oocytes were subsequently homogenized with 150 μl of solubilization buffer (20 mM Tris (pH 8.0), 10% (v/v) glycerol, 5 mM EDTA, 0.5% (v/v) Nonidet P-40, 1 mM PMSF, 10 μg/ml leupeptin, 10 μg/ml pepstatin) and incubated on ice for 1 h and centrifuged at 16,000 × *g* for 1 h at 4 °C. The solubilized proteins were added to antibody-bound beads in sucrose buffer (100 mM NaCl, 20 mM Tris (pH 8.0), 5 mM EDTA, 0.1% (v/v) Triton X-100, 10% (w/v) sucrose, 1 mM PMSF, 10 μg/ml leupeptin, 10 μg/ml pepstatin) and incubated overnight at 4 °C. Subsequently, the beads were washed with IPP100, and proteins were eluted in Laemmli as described previously (29).

Immunocytochemistry—X. laevis oocytes were injected with 5 ng of cRNA of HA-tagged TRPV5 or co-injected with 5 ng of cRNA of HA-tagged TRPV5 and 10 ng of nontagged TRPV5 mutants (TRPV5ΔC, TRPV5ΔN, and TRPV5ΔNΔC), respectively. Immunocytochemistry was performed as described previously (30, 31).

$^{45}Ca^{2+}$ Uptake Assay—X. laevis oocytes were injected with 5 ng of HA-TRPV5 cRNA only or co-injected with 10 ng of TRPV5ΔN, TRPV5ΔC or TRPV5ΔNΔC cRNA. Ca^{2+} uptake was determined 2 days after injection as described previously (2).

Plasma Membrane Isolation—X. laevis oocytes were injected with 5 ng of HA-TRPV5 cRNA only or co-injected with 5 ng of HA-TRPV5 and 10 ng of TRPV5 truncated cRNA (TRPV5ΔC, TRPV5ΔN, or TRPV5ΔNΔC). After 48 h follicle membranes were manually removed, and 12 oocytes were incubated in MBSS (20 mM MES, 80 mM NaCl, pH 6.0, containing 1% (v/v) positively charged colloidal silica (Ludox Cl, Aldrich, Bornem, Belgium)) at 4 °C for 30 min (29). Subsequently, oocytes were washed twice in MBSS and incubated with 0.1% (v/v) sodium polyacrylic acid (Aldrich) in MBSS at 4 °C for 30 min. Oocytes were homogenized in HBA buffer, and plasma membranes were isolated by serial centrifugation four times at 13.5 × *g*, two times at 24 × *g,* and two times at 38 × *g*. One-ml supernatant was exchanged with HBA buffer after each centrifugation step. Finally, membranes were pelleted at 16,000 × *g* for 30 min, dissolved in SDS sample buffer, and analyzed by immunoblotting.

RESULTS

Pull-down Assay of N-tail and C-tail of TRPV5—The role of TRPV5 N-tail and C-tail in the channel assembly was initially examined using pull-down assays. TRPV5 N-tail and C-tail were expressed as GST fusion proteins and subsequently tested for their interaction with *in vitro* translated full-length TRPV5 or the TRPV5 N-tail and C-tail. As depicted in Fig. 1*A*, the GST-fused N-tail and C-tail associated with *in vitro* translated [^{35}S]methionine-TRPV5. Moreover, pull-down analysis demonstrated N-tail-N-tail (Fig. 1*B*) and C-tail-C-tail interactions (Fig. 1*C*). To investigate whether the N-tail preferentially interacts with the N- or C-tail, the GST-N-tail was incubated with *in vitro* translated N- and C-tail simultaneously. This

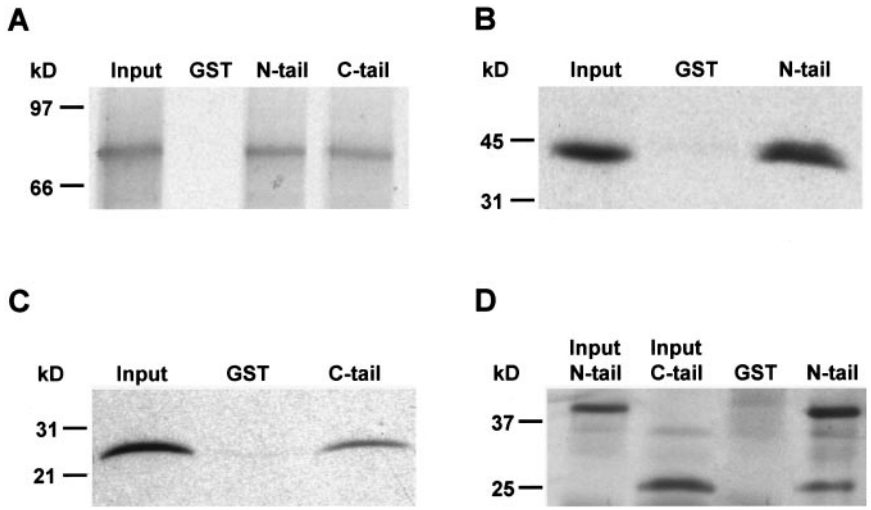

FIG. 1. **Pull-down analysis of N-tail and C-tail of TRPV5.** GST fusion proteins containing N-tail and C-tail of TRPV5 were immobilized on glutathione-Sepharose 4B beads and incubated with *in vitro* translated [^{35}S]methionine full-length TRPV5, (*A*), TRPV5 N-tail (*B*), C-tail (*C*), or both tails (*D*). The assembly was detected between *in vitro* translated full-length of TRPV5 and GST-fused TRPV5 N-tail or C-tail (*A*). Furthermore, an interaction of the N-tail with the N-tail (*B*) or the C-tail with C-tail (*C*) was observed. Incubation of the GST-N-tail with both *in vitro* translated N-tail and C-tail indicated a preference for N-N interaction rather than N-C interaction (*D*). No binding to GST alone was detected.

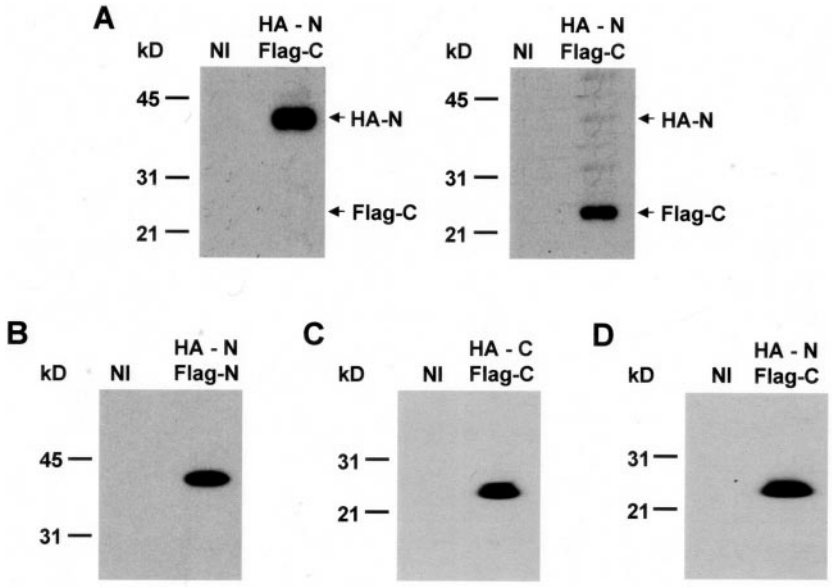

FIG. 2. **Co-immunoprecipitation of N-tail with C-tail of TRPV5.** *X. laevis* oocytes were co-injected with cRNA of HA- and FLAG-tagged N-tails, C-tails, or HA-tagged N-tail and FLAG-tagged C-tail of TRPV5, respectively. The cell lysates were processed for immunoprecipitation and immunoblot analysis. Anti-HA antibody specifically recognized HA-N-tail in total lysates from oocytes co-expressing HA-N-tail and FLAG-C-tail, whereas anti-FLAG antibody only detected the FLAG-C-tail (*A*). Subsequently, oocyte lysates were subjected to immunoprecipitation using the anti-HA antibody, and immunoblots containing protein complexes were probed with the anti-FLAG antibody. Co-immunoprecipitations were observed between HA- and FLAG-tagged N-tails (*B*), HA- and FLAG-tagged C-tails (*C*), and HA-tagged N-tail and FLAG-tagged C-tail of TRPV5 (*D*). *NI*, noninjected.

pull-down experiment indicated that the GST-N-tail preferentially binds the *in vitro* translated N-tail (Fig. 1*D*). All interactions were specific, as no interaction with GST alone was observed.

Co-immunoprecipitation of N-tail and C-tail of TRPV5—The findings from the pull-down experiments suggested that the N-tail and C-tail of TRPV5 contributed to channel assembly. Therefore, we tested whether the N-tail and C-tail of TRPV5 can be co-immunoprecipitated. First, immunoblot analysis confirmed expression of both tails that were specifically detected by the applied anti-HA or anti-FLAG antibody, respectively. The anti-HA antibody specifically detected the HA-N-tail in total lysates from oocytes co-expressing HA-N-tail and FLAG-C-tail, whereas anti-FLAG antibody only recognized the FLAG-C-tail (Fig. 2*A*). The HA- and FLAG-tagged N-tails (Fig. 2*B*), HA- and FLAG-tagged C-tails (Fig. 2*C*), or HA-N-tail with FLAG-C-tail of TRPV5 (Fig. 2*D*) were co-expressed and subsequently immunoprecipitated using the anti-HA antibody. Immunoblots containing the immune complexes were probed with the anti-FLAG antibody. Most interestingly, Fig. 2 showed that FLAG-tagged N-tail or C-tail was co-immunoprecipitated with the HA-tagged N-tail or C-tail of TRPV5, demonstrating N-N, C-C, and N-C interactions in a TRPV5 channel complex.

Functional Analysis of TRPV5 Channel Assembly—To further elucidate the functional consequences of the observed interactions between N-N tail, N-C tail, and C-C tail, the effect of co-expressing TRPV5 wild-type and truncated proteins (TRPV5ΔN, TRPV5ΔC, or TRPV5ΔNΔC) on TRPV5 activity at the plasma membrane was determined in *X. laevis* oocytes and HEK293 cells. First, oocytes were injected with HA-TRPV5 only or co-injected with TRPV5ΔN, TRPV5ΔC, or TRPV5ΔNΔC cRNA. Expression of TRPV5 resulted in ~3.5-fold increase of $^{45}Ca^{2+}$ influx compared with noninjected oocytes (Fig. 3*A*). Co-expression of TRPV5ΔN significantly decreased the TRPV5-mediated Ca^{2+} influx compared with TRPV5 alone, whereas co-expression of TRPV5ΔC completely inhibited Ca^{2+} influx to a level that was indistinguishable from noninjected oocytes. In contrast, co-expression of TRPV5ΔNΔC had no significant effect on TRPV5 channel activity (Fig. 3*A*). $^{45}Ca^{2+}$ uptake in oocytes expressing only TRPV5ΔN, TRPV5ΔC, or TRPV5ΔNΔC was not different from noninjected oocytes (data not shown). Second, patch clamp analysis was performed to investigate the electrophysiological properties of channel complexes consisting of wild-type and TRPV5 truncated proteins. Truncated channels, including TRPV5ΔN, TRPV5ΔC, and TRPV5ΔNΔC, were (co)expressed with wild-type TRPV5 in HEK293 cells. As shown in Fig. 3*B*, HEK293 cells expressing TRPV5ΔN, TRPV5ΔC or TRPV5ΔNΔC did not yield any Na^+ currents and were not different from nontransfected cells (data not shown). Remarkably, HEK293 cells co-expressing wild-type TRPV5 and

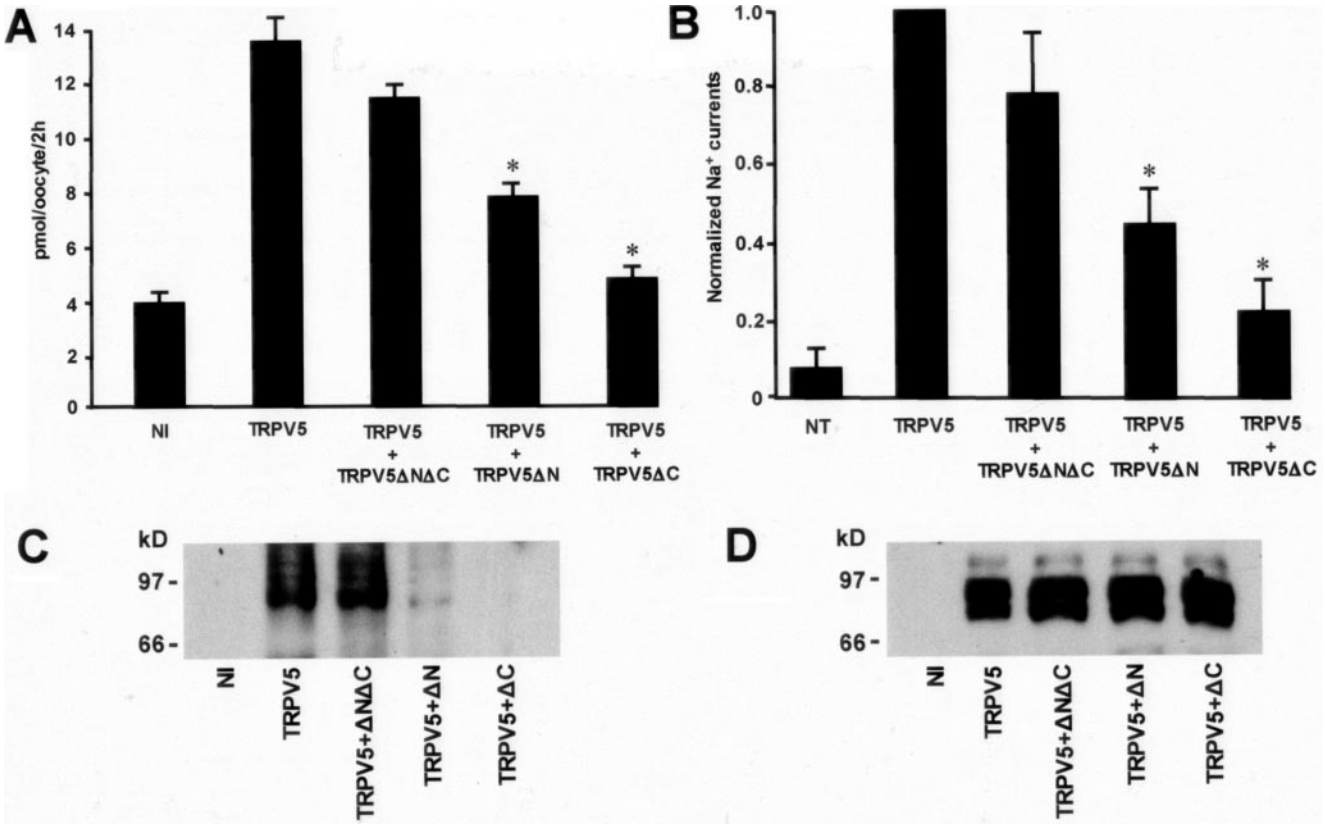

FIG. 3. **Functional analysis of TRPV5 channel assembly.** *A*, $^{45}Ca^{2+}$ uptake was measured in oocytes injected with TRPV5 cRNA only or co-injected with TRPV5ΔN, TRPV5ΔC, or TRPV5ΔNΔC cRNA. *B*, HEK293 cells were transfected with wild-type TRPV5 or TRPV5 truncated proteins, including TRPV5ΔN, TRPV5ΔC, or TRPV5ΔNΔC, or co-transfected with wild-type TRPV5 and TRPV5ΔN, TRPV5ΔC, or TRPV5ΔNΔC, and subsequently analyzed by patch clamp analysis. * indicates significance compared with TRPV5 transfected cells, $p < 0.05$. The Na^+ currents in HEK293 cells transfected with TRPV5ΔN, TRPV5ΔC, or TRPV5ΔNΔC only were not significant different from nontransfected cells (data not shown). HA-TRPV5 and truncated proteins were co-injected in *X. laevis* oocytes. To isolate plasma membrane fractions follicle membranes were removed, and plasma membranes were coated with silica. Plasma membrane fractions (*C*) or total membranes (*D*) were isolated, blotted, and analyzed for TRPV5 expression using monoclonal anti-HA antibody. *NI*, noninjected; *NT*, nontransfected.

TRPV5ΔN or TRPV5ΔC displayed significantly reduced Na^+ currents compared with wild-type TRPV5 alone. Inversely, Na^+ currents measured in HEK293 cells co-expressing wild-type TRPV5 and TRPV5ΔNΔC were not significantly affected, indicating that it is unlikely that the transmembrane domains of TRPV5 are critical determinants for subunit assembly.

TRPV5 Routing Is Disturbed by Mutant Channel Assembly—In order to understand the molecular mechanism underlying the dominant-negative effect of TRPV5 truncated proteins (TRPV5ΔN and TRPV5ΔC) on wild-type TRPV5 channel activity, a biochemical and immunocytochemical approach was combined. The expression of HA-TRPV5 was determined by analyzing plasma membrane and total membrane fractions of oocytes expressing TRPV5 alone or in combination with the truncated proteins. A distinct band at a molecular mass of ~85 kDa corresponding to the glycosylated form of TRPV5 was observed in plasma membrane fractions of TRPV5-expressing oocytes (Fig. 3*C*). Most importantly, wild-type TRPV5 expression was significantly reduced or absent in plasma membrane fractions of oocytes co-expressing TRPV5ΔN or TRPV5ΔC, respectively. However, co-injection of TRPV5ΔNΔC had no effect on the plasma membrane localization of TRPV5 (Fig. 3*C*). Most importantly, total membrane fractions showed that TRPV5 was expressed to a similar extent in the absence and presence of the TRPV5 truncated proteins (Fig. 3*D*). These results were verified by immunocytochemistry to detect TRPV5 localization on the plasma membrane. In contrast to noninjected oocytes (Fig. 4*A*), wild-type TRPV5 cRNA-injected oocytes displayed a strong immunopositive labeling along the plasma membrane,

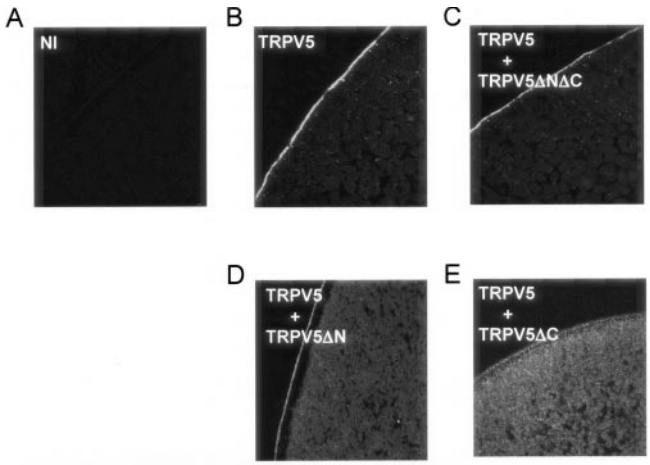

FIG. 4. **TRPV5ΔN and TRPV5ΔC expression impaired TRPV5 plasma membrane trafficking.** *X. laevis* oocytes were injected with cRNA of HA-tagged wild-type TRPV5 or co-injected with cRNA of HA-tagged wild-type TRPV5 and cRNA of nontagged TRPV5ΔN, TRPV5ΔC, or TRPV5ΔNΔC. Immunocytochemistry was performed on *X. laevis* oocytes to investigate the effect of TRPV5 truncated proteins on TRPV5 localization. Oocytes injected with wild-type TRPV5 showed predominantly immunopositive TRPV5 staining along the plasma membrane (*B*), whereas TRPV5 staining in oocytes co-expressing TRPV5ΔN (*D*) or TRPV5ΔC (*E*) was not localized at the plasma membrane but accumulated intracellularly. In addition, oocytes co-injected with wild-type TRPV5 and TRPV5ΔNΔC displayed immunopositive staining of the channel along the plasma membrane (*C*). As a negative control noninjected (*NI*) oocytes were treated in a similar way and were devoid of any staining (*A*).

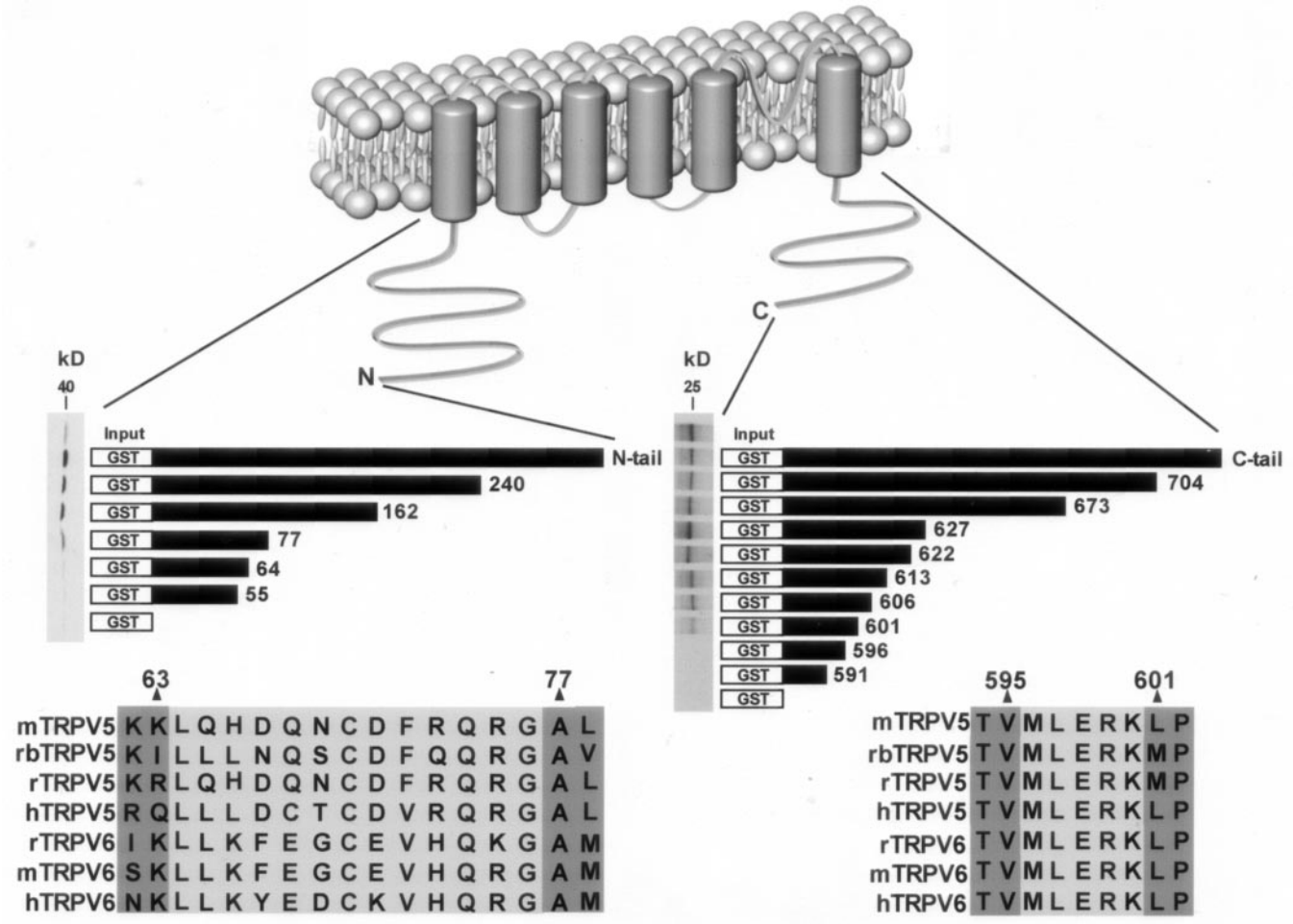

FIG. 5. **Mapping of assembly domains in TRPV5.** GST fusion proteins containing different portions of the N-tail (*left*) and C-tail (*right*) of TRPV5 were constructed according to the schematic drawing. These proteins were immobilized on glutathione-Sepharose 4B beads and then incubated with *in vitro* translated [^{35}S]methionine TRPV5 N-tail (*left*) or C-tail (*right*). Interaction of the N-tail or C-tail with the GST fusion proteins was determined by immunoblotting. The assembly domain in the N-tail was localized between residues 64 and 77 (*left*), whereas the interaction region in the C-tail (*right*) was observed between residues 596 and 601. GST was used as a negative control in the pull-down experiments. These assembly domains identified in the N- and C-tail are functionally conserved within TRPV5 and TRPV6 members as indicated by the alignments.

whereas the cytoplasm was only faintly stained (Fig. 4*B*). Most importantly, plasma membrane staining of TRPV5 was significantly decreased in oocytes co-expressing HA-TRPV5 and TRPV5ΔN and to a lesser extent HA-TRPV5 and TRPV5ΔC (Fig. 4, *D* and *E*). A strong immunopositive staining was, however, present along the plasma membrane of oocytes co-injected with HA-TRPV5 and TRPV5ΔNΔC (Fig. 4*C*). The localization of TRPV5 in the presence of TRPV5ΔN or TRPV5ΔC was predominantly intracellular. Together, these results indicated that the trafficking of HA-TRPV5 from cytosol toward the plasma membrane was disturbed by assembly with TRPV5ΔN or TRPV5ΔC, but not with TRPV5ΔNΔC, explaining the reduced channel activity. Most importantly, immunoblot analysis demonstrated that the total expression of TRPV5 was equal under all conditions (Fig. 3*D*).

Identification of the Assembly Signal in the N- and C-tail of TRPV5—To gather more detailed information regarding structural requirements for channel subunit assembly of TRPV5, a series of deletion mutants of the N- and C-tails were constructed (Fig. 5). Truncated forms of TRPV5 N-tail and C-tail were expressed as GST fusion proteins and subsequently tested for their interaction with *in vitro* translated TRPV5 N-tail and C-tail using pull-down assays. As depicted in Fig. 5 (*left part*), the interaction between GST-fused N-tail truncations and the *in vitro* translated N-tail was abolished at amino acid positions 64 and 55, whereas truncations at the positions 240 to 77 associated with *in vitro* translated N-tail. In addition, pull-down analysis demonstrated that the association of the C-tail and [^{35}S]methionine-TRPV5 C-tail disappeared when the tail was truncated at position 596, whereas truncations at position 704 to 601 did not affect the interaction (Fig. 5, *right part*). Therefore, two critical regions for TRPV5 channel assembly were located between amino acid positions 64–77 (Fig. 5, *left part*) and 596–601 (Fig. 5, *right part*) in the N- and C-tail, respectively. To elucidate further the role of the assembly domains, these regions were deleted in the N-tail (N-tailΔ64–76) and the C-tail (C-tailΔ596–600) and subsequently analyzed by pull-downs and co-immunoprecipitations as described above. First, the N-tail and the C-tail of TRPV5 were expressed as GST fusion proteins and subsequently analyzed for their interaction with *in vitro* [^{35}S]methionine translated N-tail, C-tail, and the N-tail and C-tail deletion mutants. In contrast to wild-type N-tail and C-tail, N-tailΔ64–76 and C-tailΔ596–600 did not interact with the N- and C-tail (Fig. 6*A*). Second, *X. laevis* oocytes were co-injected with wild-type and mutant HA-N-tail and FLAG-N-tail or HA-C-tail and FLAG-C-tail. Co-immunoprecipitations demonstrated that assembly between HA-N-tail/FLAG-N-tailΔ64–76, HA-N-tail/FLAG-C-tailΔ596–600, and HA-C-tail/FLAG-C-tailΔ596–600 was abolished, whereas binding between wild-type N- and C-tails was observed (Fig. 6*B*, *left*). Most importantly, both wild-type and mutant tails were equally expressed (Fig. 6*B*, *right*).

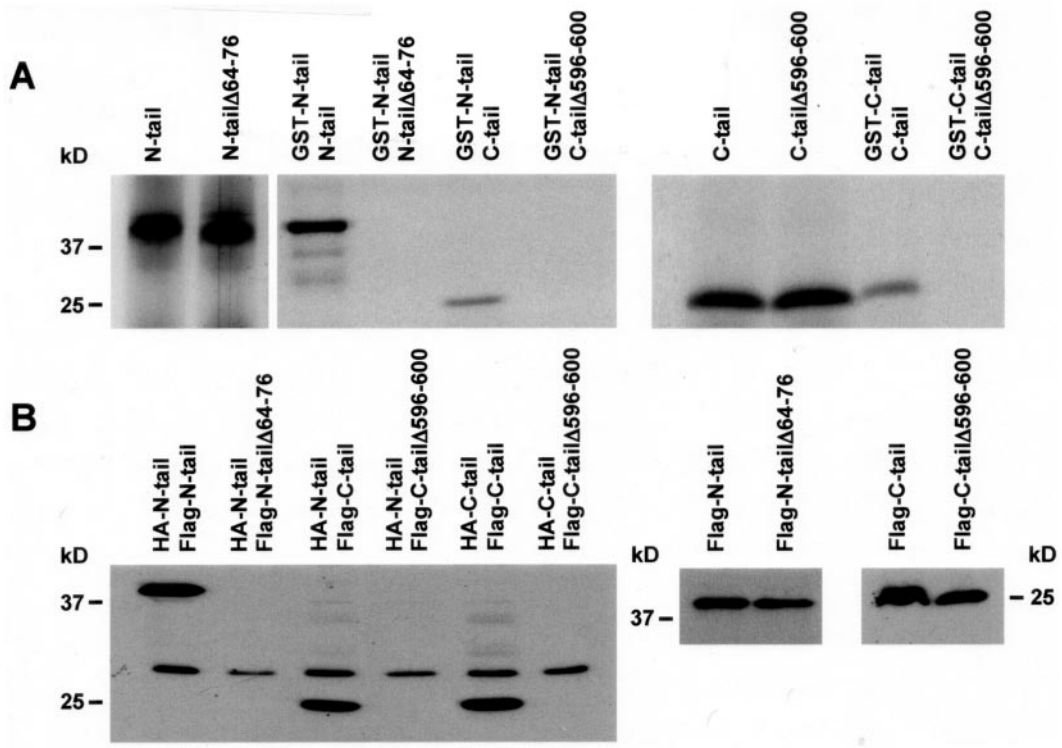

FIG. 6. **Pull-downs and co-immunoprecipitation assays of N- and C-tail deletion mutants of TRPV5.** *A*, GST fusion proteins containing the N-tail and C-tail of TRPV5 were immobilized on glutathione-Sepharose 4B beads and incubated with *in vitro* translated [^{35}S]methionine TRPV5 N-tail and C-tail or N-tail mutant lacking amino acid residues 64–76 (N-tailΔ64–76) and C-tail mutant lacking amino acid residues 596–600 (C-tailΔ596–600). *B*, *X. laevis* oocytes were co-injected with HA-N-tail and FLAG-N-tail or FLAG-N-tailΔ64–76, HA-N-tail, and FLAG-C-tail or FLAG-C-tailΔ596–600, HA-C-tail, and FLAG-C-tail or FLAG-C-tailΔ596–600, respectively. Cell lysates were processed for immunoprecipitation and immunoblotting, and subsequently protein complexes were probed with the anti-FLAG antibody. Both wild-type and mutant tails were equally expressed (*right*).

DISCUSSION

In the present study molecular determinants were identified in TRPV5 that play a key role in the formation of the functional channel complex. Using a combined approach of several independent methods, we conclude that at least two regions in the cytosolic tails of TRPV5 are important for channel assembly and subsequent routing to the plasma membrane. This conclusion is based on the following: (i) pull-down assays and co-immunoprecipitations that demonstrated physical interactions between the N-tail/N-tail, N-tail/C-tail, and C-tail/C-tail of TRPV5; (ii) $^{45}Ca^{2+}$ uptake measurements in oocytes and patch clamp analysis in HEK293 cells that showed the dominant-negative nature of TRPV5 truncated channel subunits, lacking the N-tail or C-tail, on TRPV5 wild-type channel activity; (iii) plasma membrane fractions and immunocytochemical analysis that demonstrated a disturbed trafficking of TRPV5 in oocytes co-expressing TRPV5ΔC and TRPV5ΔN toward the plasma membrane explaining the molecular mechanism of the reduced channel activity; (iv) mapping assays that revealed two critical assembly domains located at positions 64–77 in the N-tail and 596–601 in the C-tail of TRPV5; (v) deletion of these assembly domains in the N-tail and C-tail that abolished the interaction between the tails pointing to an important role of these regions in channel assembly.

By analogy with other cation channel subunits consisting of six transmembrane-spanning domains, TRP members are believed to assemble into homo- or heterotetrameric complexes. These complexes have been verified by classical methods such as co-immunoprecipitation, cross-linking analysis, or functional assays applying dominant-negative pore mutants (7–10, 32). Recently, we demonstrated a (hetero)tetrameric stoichiometry for TRPV5 and TRPV6 (32). Heterotetrameric TRPV5/6 proteins displayed properties that, depending on the subunit configuration, are intermediate between TRPV5 and TRPV6. Exchanging TRPV5 for TRPV6 subunits in a channel tetramer has major effects on Ba^{2+} permeability, Ca^{2+}-dependent inactivation, and the block by ruthenium red (32). In this way, Ca^{2+}-transporting epithelia co-expressing TRPV5 and TRPV6 may be able to generate a pleiotropic set of functional heterotetrameric channels. To date, little information is available about assembly domains in TRP proteins.

Our understanding of the architecture of functional TRP channels reflects only the end point of a complex and the poorly understood assembly pathway. Current research is beginning to elucidate the intermediate steps between the synthesis and insertion of individual subunits into the membrane. Our data indicated N-tail-N-tail and C-tail-C-tail interactions within the TRPV5 channel complexes. In addition, co-immunoprecipitations demonstrated that assembly of TRPV5 subunits occurred not only within N-tails or C-tails but also between the N-tail and C-tail. In order to further explore the crucial domains in the N-tail and C-tail for TRPV5 channel assembly, we constructed a series of truncated deletion mutants. Pull-down analysis indicated that a short peptide stretch at amino acids 64–77 is necessary for N-tail/N-tail interaction, whereas the critical region for C-tail/C-tail interaction is located between amino acids 596 and 601. Furthermore, we demonstrated by pull-down assays and co-immunoprecipitations that N- and C-tail mutants lacking these assembly domains are not able to interact with the TRPV5 tails. These findings indicated that the interaction between TRPV5 channel subunits depends on assembly signals present in the N-tail and C-tail.

It is likely that assembly also occurs within the N-tail and C-tail of TRPV6 because TRPV5 and TRPV6 share more than

75% homology at the amino acid level, raising the possibility that both N-tail and C-tail assembled together in order to form functional heterotetrameric channel complexes of TRPV5 and TRPV6 (22). Recently, Niemeyer and co-workers (33) demonstrated that the third ANK repeat within the N-tail of TRPV6 is critical for TRPV6 subunit assembly. This repeat initiates a molecular zippering process that proceeds past the fifth ANK repeat and thereby creates an intracellular anchor necessary for functional subunit assembly. In addition, deletion of this region prevented TRPV6-TRPV6 self-association and generation of functional channels (33). Pull-down mapping experiments and co-immunoprecipitations in our study identified an assembly domain in the N-tail of TRPV5 that is located more upstream, overlapping with the first ANK repeat. The most significant binding was found between the N-terminal regions 64–77. However, a slightly stronger binding signal was observed with the truncated protein at position 162 that contains the first three ANK repeats (33). These findings may suggest that the ANK repeat identified in TRPV6 could also be involved in TRPV5 channel assembly. ANK repeats have been frequently implicated in protein-protein interactions. In addition, structure prediction programs indicated that both assembly domains identified in TRPV5 participate in a predicted α-helical structure that is often engaged in protein-protein interactions to form higher order structures (34).

Detailed information about the domains involved in the process of channel subunit assembly of TRPV5 is a prerequisite for obtaining further insight into the function and properties of this channel. $^{45}Ca^{2+}$ uptake measurements demonstrated that the Ca^{2+} influx is significantly decreased or abolished in oocytes co-injected with wild-type TRPV5 and TRPV5ΔN or TRPV5ΔC, respectively. These findings are consistent with the patch clamp analysis in which the Na^+ currents were significantly reduced in HEK293 cells co-expressing wild-type TRPV5 with TRPV5ΔN or TRPV5ΔC. Plasma membrane fractions and immunocytochemistry in oocytes demonstrated the dominant-negative effect of TRPV5ΔN or TRPV5ΔC on trafficking of the wild-type TRPV5 channel to the plasma membrane. Most intriguingly, TRPV5 surface expression and activity were significantly more reduced in cells co-expressing TRPV5ΔC compared with TRPV5ΔN. This suggests a major role of the N-tail domain rather than the C-tail domain in channel assembly, which was further substantiated by pull-down experiments in which the GST-N-tail preferentially binds the N-tail compared with the C-tail. Most importantly, we demonstrated that the TRPV5 channel activity was not significantly affected in cells co-expressing wild-type TRPV5 with TRPV5ΔNΔC, which was further substantiated by a normal channel distribution on the plasma membrane of the oocyte underlining the specific involvement of the cytoplasmic tails.

Our observations are in line with the structurally related K^+ channels. The role of the N-tail in the oligomerization of Shaker K^+ subunits was first recognized by the laboratory of Jan and co-workers (35). They identified a cytoplasmic sequence preceding the first transmembrane segment that was conserved among K_{v1} subfamily members. In Shaker channels, the conserved region is found between residues 97 and 196 and is named T1 (36). Subfamily-specific assembly is provided primarily by polar interactions encoded in a conserved set of amino acids at its tetramerization interface (25). Despite the overall structural similarity between the various K^+ channel families, there appears to be little or no mixing of K^+ channel subunits between channel families (26, 35, 37–39). In the Shaker K_{v1} subfamily, the N-tail domain mediates oligomerization and prevents heteromultimer formation with members of other K_v subfamilies (35). Structures of the T1 domains of Shaker K^+ channel subfamilies provided valuable structural insights into understanding both channel assembly and functional regulation of the entire channel molecule through conformational changes (25). Most interestingly, previous studies suggested that T1 plays a role not only in channel assembly but also in channel gating and that conformational changes across the buried polar interface between subunits are a crucial part of the gating process (40). Further studies will address the question whether the identified assembly signals in TRPV5 play also a role in channel gating.

In summary, both the N-tail (amino acids 64–77) and C-tail (amino acids 596–601) are critical for TRPV5 channel assembly. Truncated TRPV5 channels at the N- or C-tail oligomerize with wild-type TRPV5 channels leading to the formation of mutant channel complexes that do not reach the plasma membrane. Therefore, assembly of channel subunits is essential for routing of the TRPV5 channel complex and subsequent activity on the plasma membrane.

REFERENCES

1. Hoenderop, J. G., Nilius, B., and Bindels, R. J. (2002) *Annu. Rev. Physiol.* **64,** 529–549
2. Hoenderop, J. G., van der Kemp, A. W., Hartog, A., van de Graaf, S. F., van Os, C. H., Willems, P. H., and Bindels, R. J. (1999) *J. Biol. Chem.* **274,** 8375–8378
3. Hoenderop, J. G., van Leeuwen, J. P., van der Eerden, B. C., Kersten, F. F., van der Kemp, A. W., Merillat, A. M., Waarsing, J. H., Rossier, B. C., Vallon, V., Hummler, E., and Bindels, R. J. (2003) *J. Clin. Investig.* **112,** 1906–1914
4. Peng, J. B., Chen, X. Z., Berger, U. V., Vassilev, P. M., Tsukaguchi, H., Brown, E. M., and Hediger, M. A. (1999) *J. Biol. Chem.* **274,** 22739–22746
5. Clapham, D. E. (2003) *Nature* **426,** 517–524
6. Bahner, M., Sander, P., Paulsen, R., and Huber, A. (2000) *J. Biol. Chem.* **275,** 2901–2904
7. Lintschinger, B., Balzer-Geldsetzer, M., Baskaran, T., Graier, W. F., Romanin, C., Zhu, M. X., and Groschner, K. (2000) *J. Biol. Chem.* **275,** 27799–27805
8. Strubing, C., Krapivinsky, G., Krapivinsky, L., and Clapham, D. E. (2001) *Neuron* **29,** 645–655
9. Hofmann, T., Schaefer, M., Schultz, G., and Gudermann, T. (2002) *Proc. Natl. Acad. Sci. U. S. A.* **99,** 7461–7466
10. Kedei, N., Szabo, T., Lile, J. D., Treanor, J. J., Olah, Z., Iadarola, M. J., and Blumberg, P. M. (2001) *J. Biol. Chem.* **276,** 28613–28619
11. Muller, D., Hoenderop, J. G., Meij, I. C., van den Heuvel, L. P., Knoers, N. V., den Hollander, A. I., Eggert, P., Garcia-Nieto, V., Claverie-Martin, F., and Bindels, R. J. (2000) *Genomics* **67,** 48–53
12. Muller, D., Hoenderop, J. G., Merkx, G. F., van Os, C. H., and Bindels, R. J. (2000) *Biochem. Biophys. Res. Commun.* **275,** 47–52
13. Weber, K., Erben, R. G., Rump, A., and Adamski, J. (2001) *Biochem. Biophys. Res. Commun.* **289,** 1287–1294
14. Nilius, B., Prenen, J., Vennekens, R., Hoenderop, J. G., Bindels, R. J., and Droogmans, G. (2001) *Cell Calcium* **29,** 417–428
15. Hoenderop, J. G., Chon, H., Gkika, D., Bluyssen, H. A., Holstege, F. C., St-Arnaud, R., Braam, B., and Bindels, R. J. (2004) *Kidney Int.* **65,** 531–539
16. Hoenderop, J. G., Dardenne, O., Van Abel, M., Van Der Kemp, A. W., Van Os, C. H., St-Arnaud, R., and Bindels, R. J. (2002) *FASEB J.* **16,** 1398–1406
17. Hoenderop, J. G., Muller, D., Van Der Kemp, A. W., Hartog, A., Suzuki, M., Ishibashi, K., Imai, M., Sweep, F., Willems, P. H., Van Os, C. H., and Bindels, R. J. (2001) *J. Am. Soc. Nephrol.* **12,** 1342–1349
18. Van Abel, M., Hoenderop, J. G., Dardenne, O., St Arnaud, R., Van Os, C. H., Van Leeuwen, H. J., and Bindels, R. J. (2002) *J. Am. Soc. Nephrol.* **13,** 2102–2109
19. van Abel, M., Hoenderop, J. G., van der Kemp, A. W., van Leeuwen, J. P., and Bindels, R. J. (2003) *Am. J. Physiol.* **285,** G78–G85
20. Van Cromphaut, S. J., Dewerchin, M., Hoenderop, J. G., Stockmans, I., Van Herck, E., Kato, S., Bindels, R. J., Collen, D., Carmeliet, P., Bouillon, R., and Carmeliet, G. (2001) *Proc. Natl. Acad. Sci. U. S. A.* **98,** 13324–13329
21. van de Graaf, S. F., Hoenderop, J. G., Gkika, D., Lamers, D., Prenen, J., Rescher, U., Gerke, V., Staub, O., Nilius, B., and Bindels, R. J. (2003) *EMBO J.* **22,** 1478–1487
22. Hoenderop, J. G., Vennekens, R., Muller, D., Prenen, J., Droogmans, G., Bindels, R. J., and Nilius, B. (2001) *J. Physiol.* (*Lond.*) **537,** 747–761
23. Lu, J., Robinson, J. M., Edwards, D., and Deutsch, C. (2001) *Biochemistry* **40,** 10934–10946
24. Shen, N. V., and Pfaffinger, P. J. (1995) *Neuron* **14,** 625–633
25. Kreusch, A., Pfaffinger, P. J., Stevens, C. F., and Choe, S. (1998) *Nature* **392,** 945–948
26. Bixby, K. A., Nanao, M. H., Shen, N. V., Kreusch, A., Bellamy, H., Pfaffinger, P. J., and Choe, S. (1999) *Nat. Struct. Biol.* **6,** 38–43
27. Steinmeyer, K., Schwappach, B., Bens, M., Vandewalle, A., and Jentsch, T. J. (1995) *J. Biol. Chem.* **270,** 31172–31177
28. Vennekens, R., Hoenderop, J. G., Prenen, J., Stuiver, M., Willems, P. H., Droogmans, G., Nilius, B., and Bindels, R. J. (2000) *J. Biol. Chem.* **275,** 3963–3969
29. Kamsteeg, E. J., Wormhoudt, T. A., Rijss, J. P., van Os, C. H., and Deen, P. M. (1999) *EMBO J.* **18,** 2394–2400
30. Mulders, S. M., Rijss, J. P., Hartog, A., Bindels, R. J., van Os, C. H., and Deen,

P. M. (1997) *Am. J. Physiol.* **273,** F451–F456
31. Mulders, S. M., Knoers, N. V., Van Lieburg, A. F., Monnens, L. A., Leumann, E., Wuhl, E., Schober, E., Rijss, J. P., Van Os, C. H., and Deen, P. M. (1997) *J. Am. Soc. Nephrol.* **8,** 242–248
32. Hoenderop, J. G., Voets, T., Hoefs, S., Weidema, F., Prenen, J., Nilius, B., and Bindels, R. J. (2003) *EMBO J.* **22,** 776–785
33. Erler, I., Hirnet, D., Wissenbach, U., Flockerzi, V., and Niemeyer, B. A. (2004) *J. Biol. Chem.* **279,** 34456–34463
34. Curran, A. R., and Engelman, D. M. (2003) *Curr. Opin. Struct. Biol.* **13,** 412–417
35. Li, M., Jan, Y. N., and Jan, L. Y. (1992) *Science* **257,** 1225–1230
36. Shen, N. V., Chen, X., Boyer, M. M., and Pfaffinger, P. J. (1993) *Neuron* **11,** 67–76
37. Covarrubias, M., Wei, A. A., and Salkoff, L. (1991) *Neuron* **7,** 763–773
38. Deal, K. K., Lovinger, D. M., and Tamkun, M. M. (1994) *J. Neurosci.* **14,** 1666–1676
39. Lee, T. E., Philipson, L. H., Kuznetsov, A., and Nelson, D. J. (1994) *Biophys. J.* **66,** 667–673
40. Minor, D. L., Lin, Y. F., Mobley, B. C., Avelar, A., Jan, Y. N., Jan, L. Y., and Berger, J. M. (2000) *Cell* **102,** 657–670